Biomacromolecules

ARTICLE

pubs.acs.org/Biomac

Polyhedral Oligomeric Silsesquioxane (POSS) Suppresses Enzymatic Degradation of PCL-Based Polyurethanes

Xinzhu Gu,[†] Jian Wu,[†] and Patrick T. Mather*

Syracuse Biomaterials Institute, Department of Biomedical and Chemical Engineering, Syracuse University, Syracuse, New York 13244, United States

Supporting Information

ABSTRACT: In this Article, we studied the enzymatic hydrolytic biodegradation behavior of a novel multiblock thermoplastic polyurethane (TPU) system, which incorporates polyhedral oligomeric silsesquioxane (POSS) into linear biodegradable thermoplastic polyurethanes containing poly(ε-caproactone) (PCL) and polyethylene glycol (PEG) blocks. The biodegradation behavior of POSS-PCL-PEG TPUs was characterized by proton nuclear magnetic resonance spectroscopy (^{1}H NMR), differential scanning calorimetry (DSC), tensile tests, scanning electron microscopy (SEM), and wavelength dispersive X-ray spectrometry (WDS) after enduring 22-day accelerated enzymatic hydrolytic degradation tests. POSS incorporation significantly suppressed in vitro enzymatic hydrolytic degradation of PCL-PEG-based multiblock TPUs by a surface passivation mechanism. WDS observations revealed that the covalently bonded POSS moieties developed a near-continuous and robust POSS-layer after initial degradation, which prevented ester bonds of PCL from enzymatic attack, thereby inhibiting further degradation. These striking results provide a new strategy to fabricate the polyester-based biostable thermoplastic polyurethanes (TPUs) of potential use in long-term surgical implants.

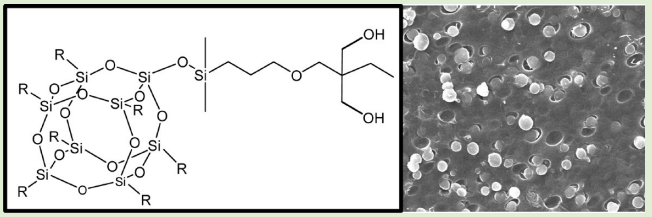

INTRODUCTION

Biostability is of critical importance for biomaterials applied for long-term medical implants and the biostability of polymeric biomaterials is of paramount importance for many applications. Thermoplastic polyurethanes (TPUs), multiblock copolymers composed of hard and soft segments, have figured prominently in the field of medical plastics for reasons discussed below. In TPUs, the hard segment block consists of a diisocyanate and a chain extender, whereas the soft segment is usually a polyol, either hydroxyl- or amine- terminated polyester, polyether, or polycarbonate. The flexible soft segment gives the TPUs great elasticity, whereas the hard segment contributes strength. Generally speaking, the two segments are incompatible with each other and tend to form a nanoscale phase-separated morphology. Because of their great potential in tailoring polymer structures, polyurethanes have unique mechanical properties and good biocompatibility that make them ideal for many implantable biomedical devices, including artificial heart components, heart valves, vascular grafts, and mammary prostheses.[1−3] The use of polyurethanes for biomedical implants was first suggested by Boretos and Pierce in 1967.[4] Since their introduction, many different polyurethanes have been evaluated for their stability in the biological environment using both in vitro and in vivo test procedures.[5−7] Nevertheless, it has been recognized that polyester-based polyurethanes are not suitable for long-term implant because of their susceptibility to hydrolytic degradation. Polyether-based polyurethanes, while hydrolytically stable, are subject to oxidative degradation.

Both poly(ε-caprolactone) (PCL) and poly(ethylene glycol) (PEG) polymers selected for incorporation within TPUs of the present study are biocompatible and nonimmunogenic. So far, there have been several PCL- or PEG-based biomedical products for various clinical uses approved by the U.S. Food and Drug Administration (FDA).[8,9] PCL is one of the most promising synthetic polymers that can degrade in contact with microorganisms.[10−12] The related enzymatic hydrolytic degradation of PCL-based polymers has also been investigated, especially in the presence of ester-bond cleavage enzymes.[13−17] Lipases are one of the most popularly studied enzymes to catalyze the cleavage of ester bonds by transesterification,[18] although they do not occur naturally in the human body. Importantly, semicrystalline PCL blocks make the associated polyurethanes stiff and hydrophobic, limiting their compatibility with soft tissues and the range of potential applications. This problem might be overcome for water-contacting applications by introducing hydrophilic blocks such as poly(ethylene glycol),[19,20] the approach adopted in our present work.

Poly(ethylene glycol) (PEG) is one of the most widely studied synthetic polymers used for designing hydrogels of use in the biomedical applications. The intrinsic hydrophilicity of PEG-based hydrogels repels nonspecific protein adsorption and resists bacterial and animal cell adhesion.[21−23] Their elastic and soft nature imparts to the TPUs low mechanical and frictional irritation when in contact with tissues and organs. However, PEG-based polyurethanes have generally exhibited poor mechanical properties.[20] The properties of these polymers can be

Received: May 20, 2011
Revised: June 14, 2011
Published: June 15, 2011

improved by either blending[24] or copolymerization.[19,25−29] Because of the combination of great advantages of PCL and PEG, PCL-PEG-based copolymers might have great potential application in biomedical fields including drug delivery, cell encapsulation, and tissue engineering.[26,28,30,31] Indeed, Skarja and Woodhouse have developed a family of biodegradable segmented polyurethanes, which has potential for use in soft tissue engineering applications.[32−34] The hard segments of these materials are composed of a phenylalanine-based diester chain extender and lysine diisocyanate, whereas the soft segments are either a PEG or PCL diol. It was found that the degradation rate and mechanical properties of these materials could be optimized by blending the PCL-based and PEG-based polyurethanes.[24] Because of its vulnerability to hydrolytic and oxidative degradation, PCL-PEG-based copolymers have proven to be unsuitable for long-term implantation. In this manuscript, we attempted to overcome this limitation through incorporation of a biostable moiety, POSS, which we now describe.

Polyhedral oligosilsesquioxane (POSS) is a class of hybrid molecules with an inorganic silicon−oxygen cage (Si_8O_{12}) and eight variable organic side groups pendant to each silicon vertex of the cage with the size of 1−3 nm. The silica-like framework renders POSS cages chemically stable, nontoxic, and mechanically robust.[35,36] Our past work on POSS polyurethanes concerned microstructure-deformation studies,[37,38] biodegradation,[39] controlled drug delivery,[40] biocompatibility,[41] and hydrogel formation.[42] Kannan et al. conducted in vitro hydrolysis and oxidation tests to assess the degradative resistance of polyhedral oligosilsesquioxane integrated poly(carbonate-urea) urethane (POSS-PCU).[43] Their studies revealed that all samples showed no significant difference in their compliance and elasticity after a 70 day hydrolysis and oxidation test, indicating striking biostability. The authors proposed that POSS nanocores covalently incorporated in PCU chains impart a type of "protective" or "shielding effect" on the soft phase, thereby preserving its elasticity and compliant properties in oxidation and hydrolysis. Polycarbonate-urethane itself, however, possesses a greater biostability than does polyether-urethane and polyester-urethane.[35,44−46] How to change the more common polyether- and polyester-based urethanes from a biodegradable form to a biostable form by incorporation of POSS (or other means) has not yet been reported.

Here we report on a series of new PCL- and PEG-based multiblock thermoplastic polyurethanes (TPUs) incorporating polyhedral oligosilsesquioxane (POSS). In this system, the POSS moieties, when covalently incorporated with PEG and PCL macromers, can be expected to aggregate and crystallize to form nanoscale crystals[42,47] induced by microphase separation due to thermodynamic incompatibility among hydrophilic PEG and hydrophobic POSS and PCL. Consequently, these crystallized moieties can become the physical cross-links of a unique hybrid hydrogel in the water-swollen state. For comparison, we also synthesized PCL-PEG TPUs without POSS, revealing the influence of POSS moieties on the enzymatic hydrolytic degradation behaviors of PCL-PEG-based TPUs in lipase solution. Moreover, we compared the influence of POSS incorporation strategies, particularly physical blending versus covalent bonding on the enzymatic degradation behaviors of TPUs.

EXPERIMENTAL SECTION

Sample Preparation. Multiblock thermoplastic polyurethanes (TPUs) were synthesized from polycaprolactone (PCL)-diol, polyethylene glycol (PEG), 2,2,4-trimethyl-1,3-pentane (TMP) POSS diol (R-group = ^{i}Bu), hereafter "POSS diol" (99.5%, Hybrid Plastics), and lysine methyl-ester diisocyanate (LDI) using a one-step technique, as shown in Scheme 1. First, PEG (1 kg/mol and 10 kg/mol, Fluka) was purified by preparing a THF solution, precipitating into n-hexane several times and then filtering. These steps were repeated several times. The purified powder was then dried in a vacuum oven at room temperature overnight. LDI (Kyowa Hakko Chemical) was purified by vacuum distillation at an oil bath temperature of 180 °C. PCL-diol (1.25 kg/mol, Sigma-Aldrich) and POSS diol were used without further purification. As a representative example, we describe the detailed procedure to prepare $[PEG_{1k}]_{50}$-$[PCL_{1k}]_{30}$-$[POSS]_{20}$ from PEG 1 kg/mol, PCL1.25 kg/mol, and POSS diol. In a 100 mL three-necked flask, 1.25 g (1.188 mmol) POSS-diol, 1.875 g (1.5 mmol) PCL diol, and 3.0 g (3 mmol) PEG were dissolved in toluene (Fisher, ACS Certified), which had been dried with the aid of calcium hydride (CaH_2, Aldrich). Under the protection of a nitrogen purge, the flask was heated to 50 °C, and a 1.04 mL (5.688 mmol) of purified LDI (ρ = 1.157 g/mL) was added to the 10 wt % toluene solution. The reaction mixture was further heated to 90 °C, and several drops of dibutyltin dilaurate catalyst (Sigma-Aldrich) were added through a syringe. The reaction was kept at 90 °C for ca. 6 h under the nitrogen purge, and a distinct viscosity rise was observed. The polymer solution was then precipitated into an excess of *n*-hexane and washed with deionized water several times to remove any unreacted PEG. PCL (42 kg/mol, Aldrich) was purchased and used as a control for the enzymatic degradation experiments.

The nomenclature used here to designate this family of multiblock thermoplastic polyurethanes (TPUs) indicates the molecular weight of the PEG and PCL chains as suffixes, whereas the subscripts indicate the feed weight percent for each segment. Therefore, $[PEG_{1k}]_{50}$-$[PCL_{1k}]_{30}$-$[POSS]_{20}$ designates, for example, a multiblock copolymer, consisting of PEG1k, PCL1k, and POSS blocks. Their feed weight percent is 50:30:20. Because POSS molecular weight remains the same for all of the polymers, it is not designated in the sample nomenclature of this Article.

The POSS TPUs obtained from synthesis and precipitation were cast from THF solution, as indicated in the following example: the polymer (1.5 g) was dissolved in THF (10 mL) and poured in a PTFE casting dish with a diameter of 10.5 cm, then transferred to a chamber to allow for a slow solvent evaporation. Following 48 h of evaporation at room atmosphere, the films (still in the dish) were put in a vacuum at room temperature for 3 to 4 days to remove any residual solvent. The resulting films were flexible, optically clear, and 0.20 mm in thickness, the latter being determined by a digital caliper. For comparison, we prepared a sample with the same loading level of POSS but without covalent tethering. Thus, we physically blended $[PEG_{10k}]_{50}$-$[PCL_{1k}]_{50}$ and POSS ($[PEG_{10k}]_{50}$-$[PCL_{1k}]_{50}$+20% POSS) in THF and then cast the blended solution in a PTFE casting dish. The drying procedure was the same as described above for other samples.

In vitro enzymatic degradation experiments were carried out at 37 °C in pH 7.0 PBS buffer containing 0.05% Tween-20 and 0.4 mg/mL Amano lipase PS from *Pseudomonas cepacia* (Aldrich). Samples with dimensions of 15 (length) × 5 (width) × 0.2 mm (thickness) were cut from a cast film. Sodium azide was added to the buffer to prevent microorganism growth. Each sample was placed into an individual vial (20 mL) containing 5 mL of buffer solution. The buffer was changed every other day with a fresh buffer solution to maintain enzyme activity. At predetermined degradation time points, three samples were removed from the buffer, washed with deionized water, patted dry, and weighed. After drying under vacuum at room temperature for 3 to 4 days, samples were reweighed to determine total percentage of mass loss. Mass percent remaining and water uptake were

Scheme 1. Preparation of PCL-PEG-POSS Multi-Block TPUs by Reacting the PEG Diol and PCL Diol with a Lysine-Derived Diisocyanate and POSS Diol

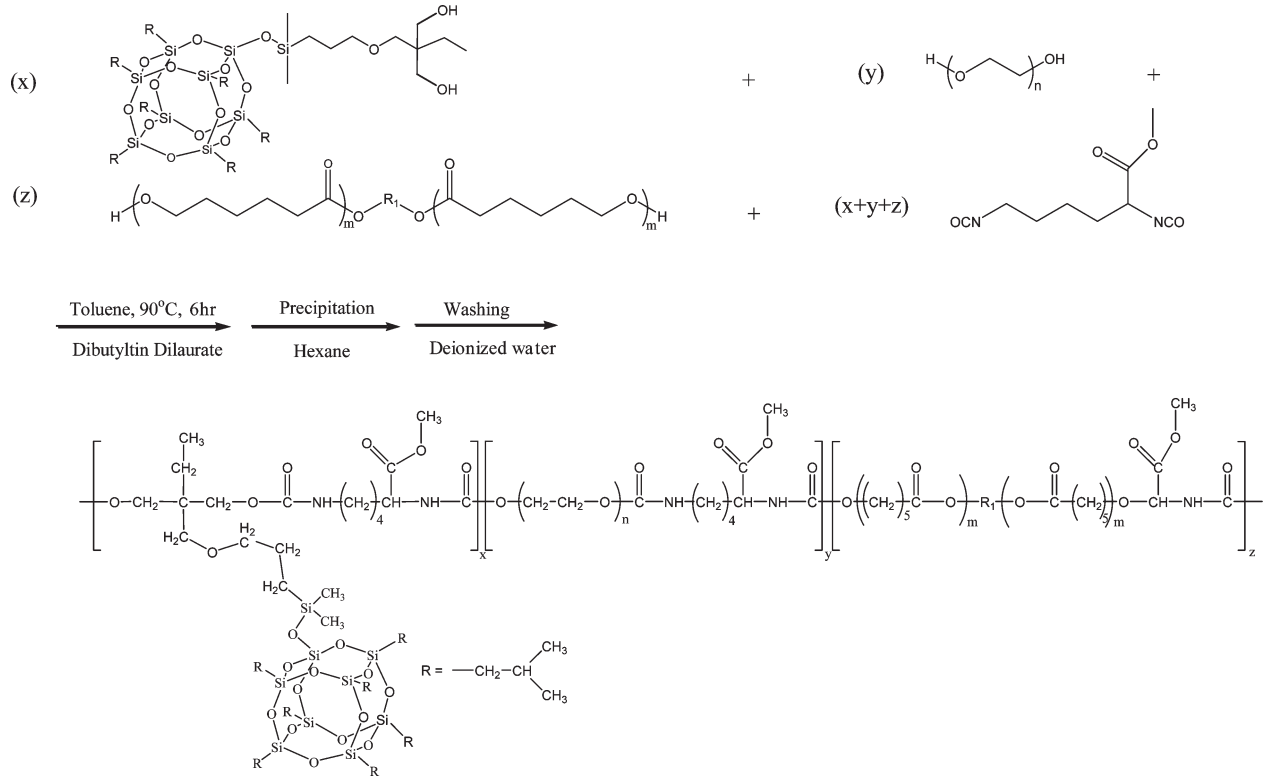

Table 1. Chemical Properties of PCL-PEG-Based Multiblock TPUs, Which Are Physically or Covalently Bonded with POSS Moieties, Including PCL-PEG TPUs and $[PCL_{42k}]_{100}$ as Controls[a]

materials	PEG/PCL/POSS feed ratio, w/w/w (mol/mol/mol)	PEG/PCL/POSS actual ratio, w/w/w (mol/mol/mol)[b]	M_n (kg/mol)[c]	PDI
$[PCL_{42k}]_{100}$	0/100/0 (0/100/0)	0/100/0 (0/100/0)	65.2	1.18
$[PEG_{10k}]_{50}$-$[PCL_{4k}]_{50}$	50/50/0 (11/89/0)	51/49/0 (11/89/0)	100.8	1.22
$[PEG_{10k}]_{50}$-$[PCL_{4k}]_{50}$+20 wt % POSS	40/40/20 (7/57/36)	37/35/28 (6/48/46)		
$[PEG_{1k}]_{50}$-$[PCL_{1k}]_{30}$-$[POSS]_{20}$	50/30/20 (56/22/22)	50/29/21 (56/22/22)	217.4	1.19
$[PEG_{10k}]_{50}$-$[PCL_{1k}]_{30}$-$[POSS]_{20}$	50/30/20 (11/44/44)	61/24/15 (16/49/35)	51.9	1.08

[a] Subscript numbers represent the block weight %. [b] Based on ^{1}H NMR. [c] Based on light scattering from GPC.

calculated using the following equations

$$\text{mass remaining } (\%) = \left(\frac{m_d}{m_{orig}}\right) \times 100 \quad (1)$$

$$\text{water uptake } (\%) = \left(\frac{m_w - m_d}{m_d}\right) \times 100 \quad (2)$$

where m_d is the sample after drying under vacuum, m_{orig} is the mass of the initial, nondegraded sample, and m_w is the mass of the wet sample. Average values for three samples are reported herein, with the error bars indicating one standard deviation. All of the samples were vacuum-dried for 1 week before being subjected to further analysis.

Polymer Characterization. Analysis of molecular weight before and during degradation was performed using gel permeation chromatography (GPC) with a Waters Isocratic HPLC system equipped with a temperature-controlled differential refractometer (Waters 2414). Multi-angle laser light scattering was employed (Wyatt miniDAWN) using three angles (45, 90, 135°) of scattered light detection to allow absolute molecular weight determination. Samples were dissolved in THF at a

Table 2. Material Properties of PCL-PEG-Based Multiblock TPUs and $[PCL_{42k}]_{100}$

materials	T_g (°C)	T_m^{PEG} (°C) [$\Delta H_{m,PEG}$ (J/g)]	T_m^{POSS} (°C) [$\Delta H_{m,POSS}$ (J/g)]	T_m^{PCL} (°C) [$\Delta H_{m,PCL}$ (J/g)]	water uptake (%)
$[PCL_{42k}]_{100}$	−62.5			55.2 [60.7]	0
$[PEG_{10k}]_{50}$-$[PCL_{1k}]_{50}$	−48.7	48.9 [61.8]		24.7 [0.4]	179.1
$[PEG_{10k}]_{50}$-$[PCL_{1k}]_{50}$ + 20 wt % POSS	−49.9	49.6 [48.6]	123.1 [4.4]		164.4
$[PEG_{1k}]_{50}$-$[PCL_{1k}]_{30}$-$[POSS]_{20}$	−48.2		107.0 [1.9]		70.7
$[PEG_{10k}]_{50}$-$[PCL_{1k}]_{30}$-$[POSS]_{20}$	−48.1	46.5 [50.1]	117.5 [1.4]		182.0

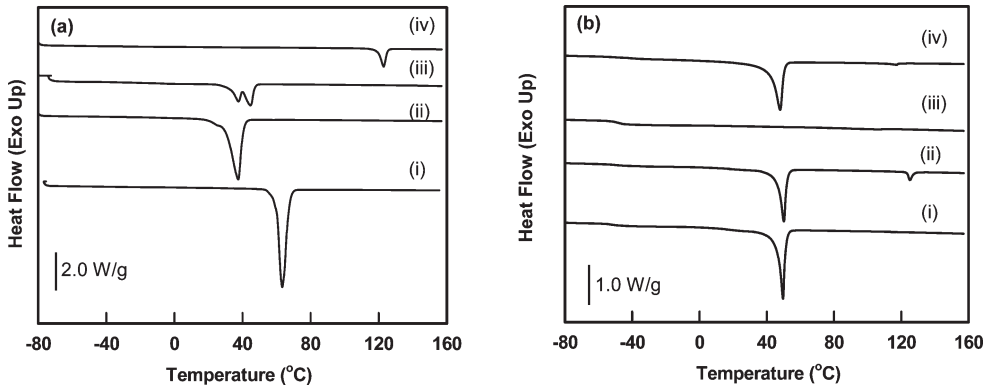

Figure 1. DSC second heating traces for: (a) diols used to synthesize PCL-PEG-based TPUs: (i) PEG10k, (ii) PEG1k, (iii) PCL1k-diol, and (iv) POSS-diol and (b) PCL-PEG-based TPUs (i) $[PEG_{10k}]_{50}$-$[PCL_{1k}]_{50}$, (ii) $[PEG_{10k}]_{50}$-$[PCL_{1k}]_{50}$ +20 wt % POSS, (iii) $[PEG_{1k}]_{50}$-$[PCL_{1k}]_{30}$-$[POSS]_{20}$, and (iv) $[PEG_{10k}]_{50}$-$[PCL_{1k}]_{30}$-$[POSS]_{20}$.

concentration of ~2 mg/mL and were passed through a 0.2 μm PTFE filter prior to injection. The GPC was operated at a flow rate of 1 mL/min.

Chemical compositions of the final products were determined by liquid-phase proton nuclear magnetic resonance spectroscopy (^{1}H NMR) using methods described in prior work.[39] Samples were dissolved in deuterated chloroform ($CDCl_3$) and were analyzed by performing 24 scans per sample using a 300 MHz Bruker Avance spectrometer.

Phase behavior and thermal transitions of TPUs were determined by differential scanning calorimetry (DSC, TA Instruments Q200) under continuous nitrogen purge (50 mL/min). The samples were made by encapsulating ~3 to 5 mg of polymer in a TA Instruments aluminum pan. The heating and cooling rate for each sample was 10 °C/min. After annealing each sample at 160 °C for 5 min to melt residual POSS crystals, the samples were cooled to −85 °C and then heated again to 160 °C at the same heating rate. The data reported here are from second heating runs unless otherwise mentioned. Glass-transition temperatures (T_g) were taken as the midpoint of the stepwise decrease in the heat flow trace observed during heating. Melting points were taken as the temperatures corresponding to the valley (peak) of the endothermic transition during the second heat, with heats-of-fusion (ΔH) being determined through integration of that peak and normalization for the sample mass.

To determine the microstructures of the thermoplastic polyurethane (TPU) films, we conducted wide-angle X-ray scattering (WAXS) by employing Rigaku S-MAX3000 (Woodlands, TX) in transmission mode. A FujiFilm FLA7000 reader and a Fujifilm IP Eraser 3 were used to collect the scattered X-ray patterns. A Rigaku generator (MicroMax-002$^+$) was employed to produce a Cu K_α radiation with the wavelength of 1.5405 Å. An accelerating voltage of 45 kV and a current of 0.88 mA were applied. The distance between sample and image plate was fixed at 120 mm for wide-angle X-ray scattering collection. The resulting scattering angular was in range of $5° < 2\theta < 40°$. The WAXS profiles of the sample were collected without background subtraction, benefiting from the fact that the whole X-ray system was run under a high vacuum condition.

The water swelling behavior of the TPUs was studied by a gravimetric procedure. The dried samples were cut into rectangular pieces, each with a mass of ~10 mg, and were immersed in Millipore-purified water for 12 h to equilibrate the water uptake. Then, the samples were removed from the water, patted dry, and weighed again. Water uptake measurements were quantified using eq 2. All reported values represent the average of two samples.

The mechanical properties of samples before and after prescribed periods of enzymatic degradation were evaluated by uniaxial tensile testing employing Linkam TST 350 (Linkam Scientific Instruments; 20 N load cell, 0.01 N resolution) tensile testing system at room temperature. The polymer films were punched into a dogbone geometry using a dogbone die (TestResources; machined tool steel), a press (Carver, model C), and minimal pressure. The dimensions of the dogbone die were determined from a scaled down D638-03 type IV ASTM standard and had a width of 1.5 mm, gauge length of 6.25 mm, and total length of 28.75 mm. Samples were extensionally deformed at

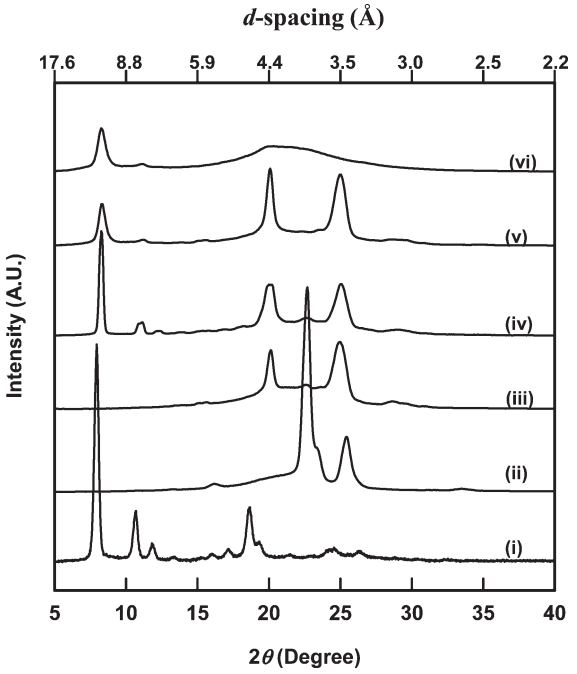

Figure 2. WAXS patterns of PCL-PEG-based TPUs incorporating POSS moieties indicated in Table 1: (i) POSS-diol monomer, (ii) $[PCL_{42k}]_{100}$, (iii) $[PEG_{10k}]_{50}$-$[PCL_{1k}]_{50}$, (iv) $[PEG_{10k}]_{50}$-$[PCL_{1k}]_{50}$ + 20 wt % POSS, (v) $[PEG_{10k}]_{50}$-$[PCL_{1k}]_{30}$-$[POSS]_{20}$, and (vi) $[PEG_{1k}]_{50}$-$[PCL_{1k}]_{30}$-$[POSS]_{20}$. The X-ray wavelength (λ) is 1.5405 Å.

crosshead speed of 200 μm/s (192%/min). This experiment was conducted three times per material. Young's modulus was calculated by finding the initial slope of the stress versus strain curve ($0 < \varepsilon < 8\%$) using linear regression. The yield stress was determined by the maximum stress following the proportional limit and the strain-at-break recorded as the strain at the point where the force became zero (after elongation).

Mechanical properties of the materials after degradation were determined using a dynamic mechanical analyzer (TA Instruments, Q800) in tensile testing mode with a displacement rate of 1.0 mm/min (160%/min). Samples were cut from both the as-cast films and the degraded films with the typical dimensions of 9 mm (length) × 1.5 mm (width) × 0.2 mm (thickness). Each experiment was repeated three times, with typical results presented graphically and average analyzed results tabulated.

The surface morphologies of all films before and after enzymatic degradation were investigated using scanning electron microscopy (SEM; JEOL, JSM-5600). All of the samples were first coated with gold for 60 s using an Enton Vacuum-Desk II gold sputter-coater to yield coating thickness of ~200 Å, suitable for SEM observation without charge accumulation.

A JEOL 8600 electron microprobe equipped with five wavelength dispersive X-ray spectrometers (WDS) was used to analyze quantitatively the elemental composition of sample surfaces before and after degradation. The JEOL8600 was equipped with the Geller Microanalytical Hardware/Software automation package. Films were coated with gold using the same methods as described for SEM samples. High-resolution element maps for silicon were generated for each sample to show the relative Si concentration within one sample. The acquisition time for each map was 1 h. In our micrograph representations, brighter fields represent higher silicon concentration. For each sample, 10 different locations were scanned, and the concentration of silicon was calculated. The accelerating voltage, the filament current, and the probe current are 10 kV, 240 mA, and 5.4 nA, respectively, each held constant during the whole experiment. The fixed working distance between the sample and pole piece of the JEOL 8600 was 11 mm.

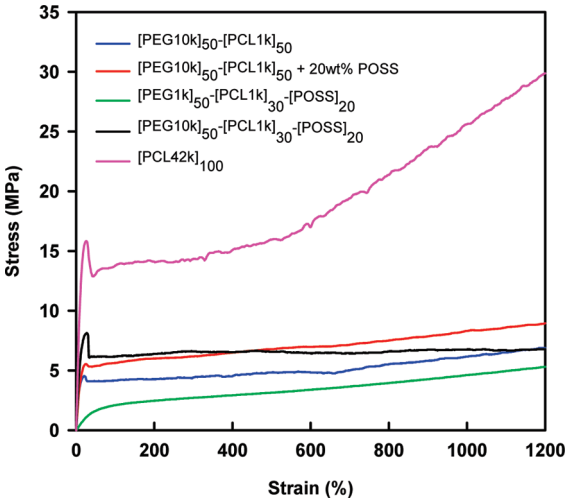

Figure 3. Stress−strain response of PCL-PEG-based multiblock TPUs and $[PCL_{42k}]_{100}$.

RESULTS AND DISCUSSION

Characterization of Multiblock Thermoplastic Polyurethanes. The number-average molecular weight and molecular weight distributions of the hybrid polyurethanes and pure commercial PCL are detailed in Table 1. The molecular weight of the synthesized polymers varied in the range of 51.9−217.4 kg/mol, and their corresponding molecular weight polydispersities varied from 1.08 to 1.22, which are relatively narrow for addition polymerization and are attributed to the precipitation process leading naturally to fractionation. ^{1}H NMR analysis was used to determine quantitatively the molar ratio of PEG/PCL/POSS by comparing the integration value of proton signal of POSS macromers at δ 0.12 ($-O-Si(CH_3)_2-CH_2-$), that of PEG at δ 3.65 ($-CH_2-CH_2-O-$), and that of PCL at δ 2.32 ($-(C=O)-(CH_2)_4-CH_2-O-$). Before comparison, all of the integration values were normalized to those for a single proton. For reactions in which POSS was included, the POSS/PCL/PEG feed ratio, as indicated by the final number in each polymer's naming scheme, was not always what was observed in the resulting product. In $[PEG_{10k}]_{50}$-$[PCL_{1k}]_{30}$-$[POSS]_{20}$, for example, the lowered POSS and PCL inclusion most likely results from higher reactivity of PEG 10k blocks compared with POSS and PCL1k blocks. A sample ^{1}H NMR spectrum, $[PEG_{10k}]_{50}$-$[PCL_{1k}]_{30}$-$[POSS]_{20}$, along with characteristic peak assignments, can be found in the Supporting Information (Figure S1).

Thermal behavior of the TPUs and $[PCL_{42k}]_{100}$ are summarized in Table 2, and the second heating curves for all TPUs and diols are shown in Figure 1. All TPUs showed very similar glass-transition temperatures (T_g) ranging from −48.1 to −49.9 °C. The melting peak of $[PEG_{10k}]_{50}$-$[PCL_{1k}]_{50}$ at 48.9 °C is ascribed to PEG-rich domains, which is lower than the pure PEG10k (63.4 °C). The small melting peak at 25 °C is assigned to PCL domain, where PCL blocks are sufficiently long to crystallize and are also able to hamper substantially PEG crystallization. These results were in agreement with what has been obtained by other researchers for multiblock copolymers containing PEG

Table 3. Mechanical Properties of PCL-PEG-Based Multiblock TPUs and $[PCL_{42k}]_{100}$

materials	Young's moduli (MPa)	yield stress (MPa)	yield strain (%)	elongation at break (%)
$[LPCL_{42k}]_{100}$	130.0 ± 14.1	16.4 ± 3.4	24.5 ± 1.0	>1200
$[PEG_{10k}]_{50}$-$[PCL_{1k}]_{50}$	44.9 ± 4.4	4.6 ± 0.1	23.5 ± 1.0	>1200
$[PEG_{10k}]_{50}$-$[PCL_{1k}]_{50}$ + 20 wt % POSS	46.4 ± 3.7	5.5 ± 0.6	17.1 ± 4.8	>1200
$[PEG_{1k}]_{50}$-$[PCL_{4k}]_{30}$-$[POSS]_{20}$	4.9 ± 0.8			>1200
$[PEG_{10k}]_{50}$-$[PCL_{4k}]_{30}$-$[POSS]_{20}$	69.3 ± 4.1	7.6 ± 0.5	23.0 ± 3.8	>1200

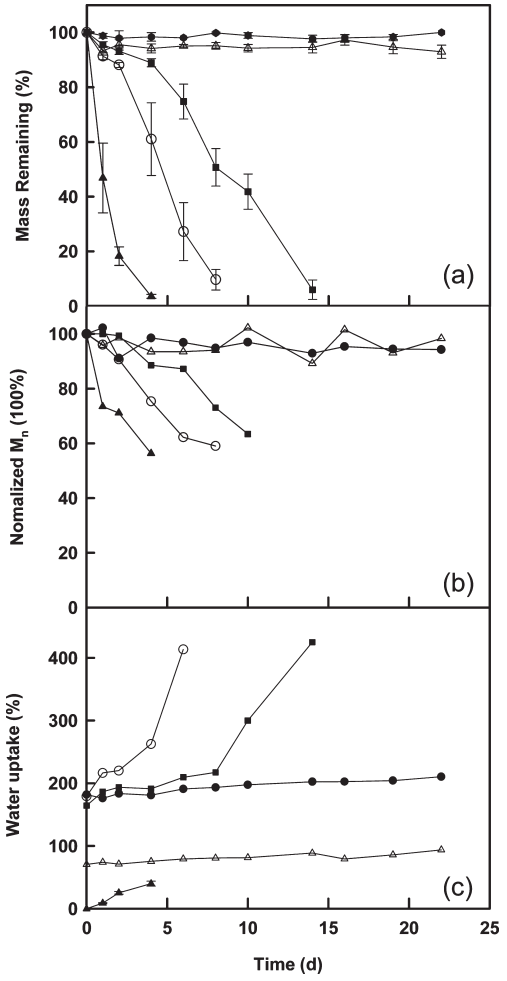

Figure 4. (a) Mass remaining profiles, (b) normalized number-average molecular weight (M_n) remaining profiles, and (c) water uptake profiles of PCL-PEG-based multiblock TPUs and $[PCL_{42k}]_{100}$ during enzymatic degradation by Lipase PS (0.4 mg/mL) in a pH 7.4 PBS solution at 37 °C. $[PEG_{10k}]_{50}$-$[PCL_{1k}]_{50}$ (○), $[PEG_{10k}]_{50}$-$[PCL_{1k}]_{50}$ + 20 wt % POSS (■), $[PEG_{1k}]_{50}$-$[PCL_{1k}]_{30}$-$[POSS]_{20}$ (△), $[PEG_{10k}]_{50}$-$[PCL_{1k}]_{30}$-$[POSS]_{20}$ (●), and $[PCL_{42k}]_{100}$ (▲).

and PCL.[25,29] In TPUs, PEG and PCL blocks are immiscible with each other and form individual domains.[48] After being physically blended with 20 wt % POSS-diol macromer by solution casting, $[PEG_{10k}]_{50}$-$[PCL_{1k}]_{50}$ + 20% POSS gained a higher melting point of 123.1 °C, which is very close to the pure POSS-diol T_m at 122 °C. We interpret this to mean that the unbounded POSS macromer is immiscible with the multiblock TPUs prepared from PCL-diol and PEG-diol building blocks. In contrast, $[PEG_{1k}]_{50}$-$[PCL_{1k}]_{30}$-$[POSS]_{20}$, in which POSS was covalently bonded with PCL-PEG, showed only one endothermic peak

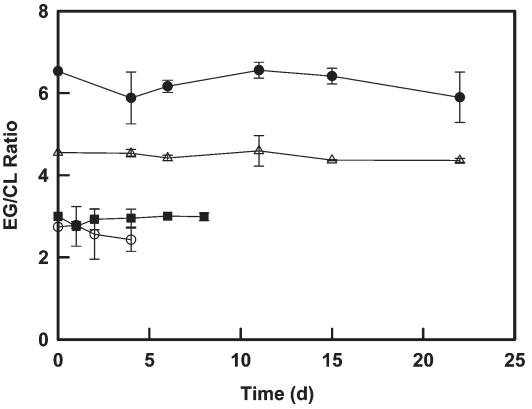

Figure 5. EG/CL ratios of PCL-PEG-based multiblock TPUs during enzymatic degradation, determined by ^{1}H NMR. $[PEG_{10k}]_{50}$-$[PCL_{1k}]_{50}$ (○); $[PEG_{10k}]_{50}$-$[PCL_{1k}]_{50}$ + 20 wt % POSS (■); $[PEG_{1k}]_{50}$-$[PCL_{1k}]_{30}$-$[POSS]_{20}$ (△); and $[PEG_{10k}]_{50}$-$[PCL_{1k}]_{30}$-$[POSS]_{20}$ (●).

at (107.0 °C), indicating that both PEG (1 kg/mol) and PCL (1.25 kg/mol) blocks are amorphous. The melting point and the melting enthalpy of POSS-diol were found to be lower in the two multiblock TPUs covalently incorporating POSS moieties ($[PEG_{10k}]_{50}$-$[PCL_{1k}]_{30}$-$[POSS]_{20}$ and $[PEG_{1k}]_{50}$-$[PCL_{1k}]_{30}$-$[POSS]_{20}$) than in the $[PEG_{10k}]_{50}$-$[PCL_{1k}]_{50}$ + 20% POSS blend. We reason that in the physically blended system, POSS has more freedom to diffuse and crystallize into 3D crystals without constraint from the covalent tether to the polymer backbone, so the resulting POSS crystallites have a relatively larger size and higher crystallinity. DSC second heating traces for PCL-PEG-based TPUs showing POSS melting peaks are displayed in Figure S2 of the Supporting Information.

Wide-angle X-ray scattering was conducted to determine the microstructures of the multiblock thermoplastic polyurethane (TPU) films. For pure POSS-diol monomer, there are three characteristic diffraction peaks shown in Figure 2. They are centered at d spacing of 11.1 (2θ = 7.9°), 8.3 (2θ = 10.6°), and 4.8 Å (2θ = 18.6°), which are quite similar with our previous observations for the polylactide—POSS system.[39] For pure PCL with M_n = 42 kg/mol, we observed two strong characteristic diffraction peaks centered at d spacing of 4.0 (2θ = 22.5°) and 3.6 Å (2θ = 25.0°), both of which can be assigned to 110 and 200 reflection peaks of PCL orthorhombic unit cell. However, these two characteristic diffraction peaks become very weak in $[PEG_{10k}]_{50}$-$[PCL_{1k}]_{50}$, which incorporates low-molecular-weight PCL-diol (1.25 kg/mol) and high-molecular-weight PEG-diol (10 kg/mol). As shown in Figure 2, trace iii, there is only one weak observable diffraction peak ascribed to PCL crystalline domain centered at 4.0 Å, and two strong characteristic peaks entered at d spacing of 4.5 (2θ = 19.9°) and 3.7 Å (2θ = 24.3°), both of which

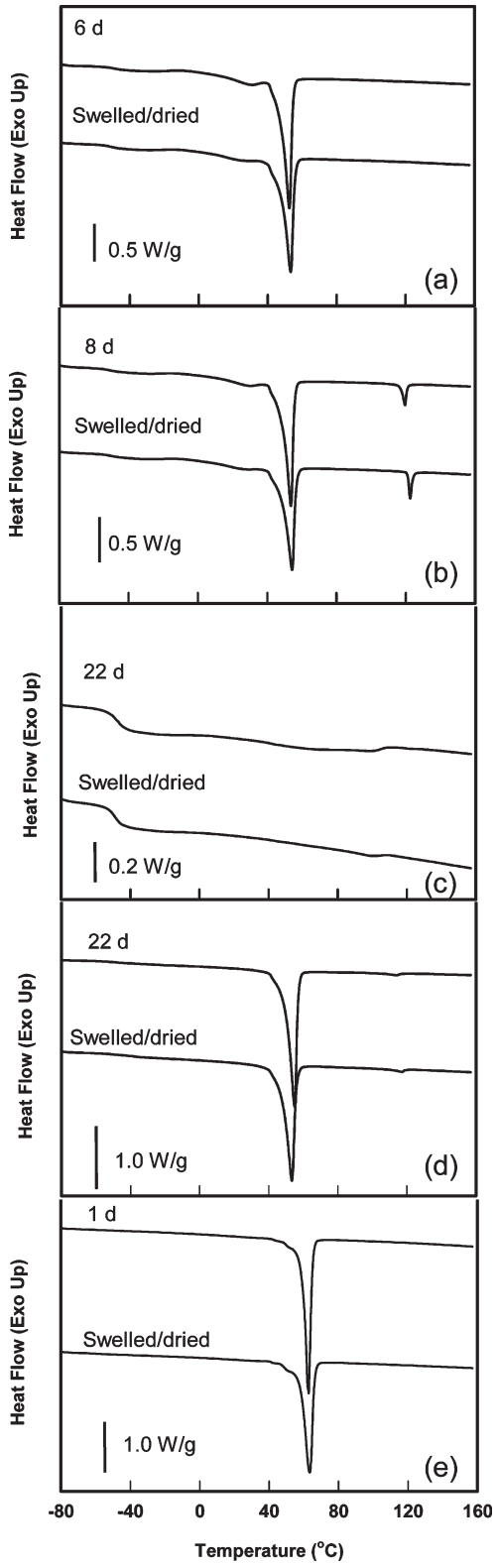

Figure 6. DSC first heating traces for (a) $[PEG_{10k}]_{50}$-$[PCL_{1k}]_{50}$, (b) $[PEG_{10k}]_{50}$-$[PCL_{1k}]_{50}$ + 20 wt % POSS, (c) $[PEG_{1k}]_{50}$-$[PCL_{1k}]_{30}$-$[POSS]_{20}$, (d) $[PEG_{10k}]_{50}$-$[PCL_{1k}]_{30}$-$[POSS]_{20}$, and (e) $[PCL_{42k}]_{100}$ before and after enzymatic degradation.

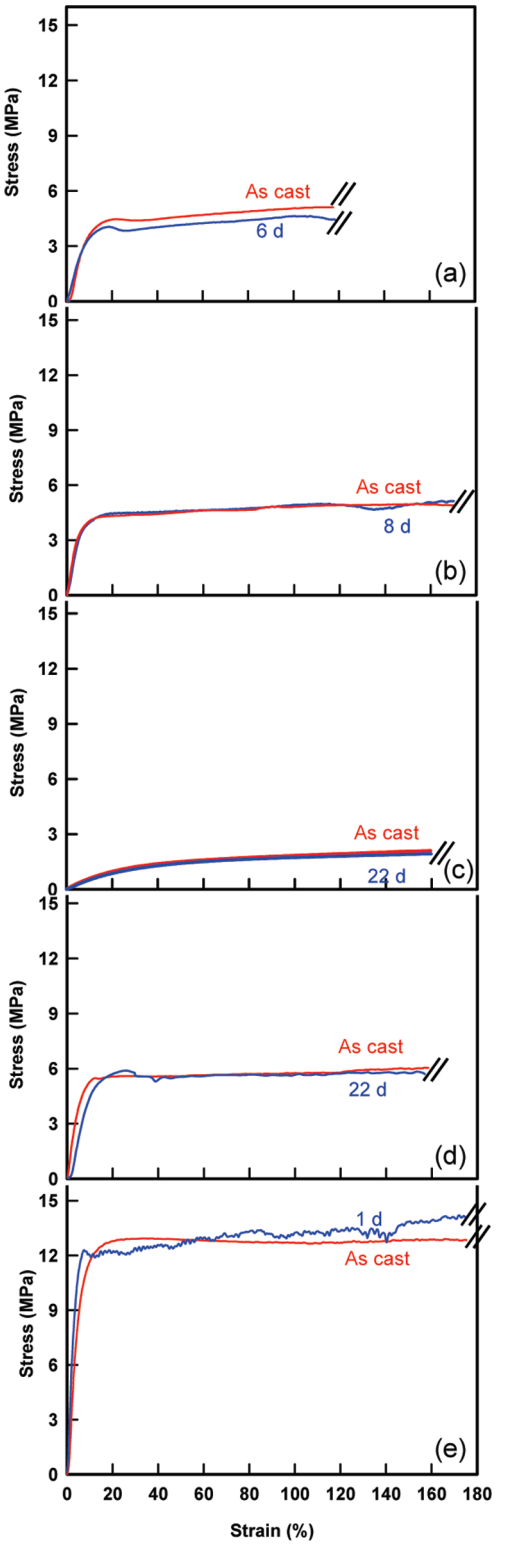

Figure 7. Stress−strain curves for (a) $[PEG_{10k}]_{50}$-$[PCL_{1k}]_{50}$, (b) $[PEG_{10k}]_{50}$-$[PCL_{1k}]_{50}$ + 20 wt % POSS, (c) $[PEG_{1k}]_{50}$-$[PCL_{1k}]_{30}$-$[POSS]_{20}$, (d) $[PEG_{10k}]_{50}$-$[PCL_{1k}]_{30}$-$[POSS]_{20}$, and (e) $[PCL_{42k}]_{100}$ before and after enzymatic degradation.

can be ascribed to 120 and $1\bar{3}2$ reflection peaks of PEG monoclinic unit cell, respectively. Clearly, the hydrophilic segment of PEG and hydrophobic PCL each can form independent crystalline microstructures indicating microphase separation due to thermodynamic incompatibility, although the diffraction peak related to PCL

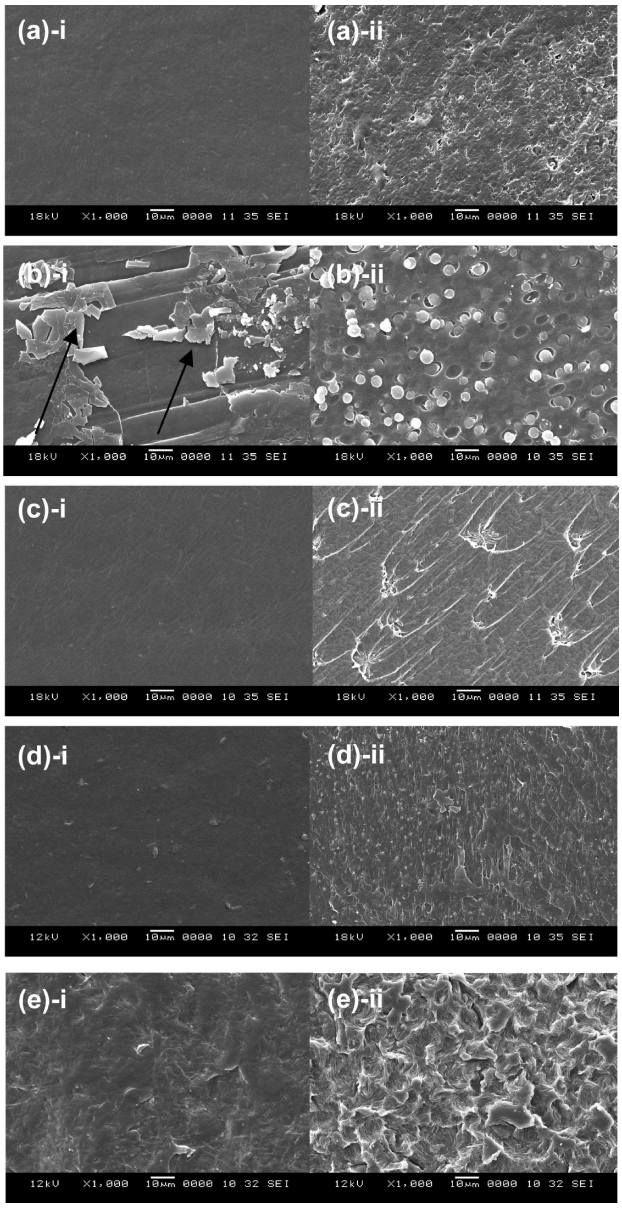

Figure 8. SEM images of: (a) $[PEG_{10k}]_{50}$-$[PCL_{1k}]_{50}$: (i) swelled/dried and (ii) in lipase buffer for 6 days; (b) $[PEG_{10k}]_{50}$-$[PCL_{1k}]_{50}$ + 20 wt % POSS: (i) swelled/dried and (ii) in lipase buffer for 10 days; (c) $[PEG_{1k}]_{50}$-$[PCL_{1k}]_{30}$-$[POSS]_{20}$: (i) swelled/dried and (ii) in lipase buffer for 22 days; (d) $[PEG_{10k}]_{50}$-$[PCL_{1k}]_{30}$-$[POSS]_{20}$: (i) swelled/dried and (ii) in lipase buffer for 22 days; and (e) $[PCL_{42k}]_{100}$: (i) swelled/dried and (ii) in lipase buffer for 1 day.

crystalline domain is weak because of the low molecular weight of the PCL-diol building block.

After solvent-blending with 20 wt % POSS-diol macromer, $[PEG_{10k}]_{50}$-$[PCL_{1k}]_{50}$ + 20% POSS blend gained a third strong characteristic peak centered at d spacing of 10.7 Å ($2\theta = 8.3°$), as shown in trace (iv) of Figure 2. This further confirmed that POSS macromer is immiscible with the multiblock TPUs prepared from PCL-diol and PEG-diol segments and forms discrete POSS-rich crystalline domains. Notably, this peak in the TPUs is shifted slightly to a larger diffraction angle ($2\theta = 8.3°$, d spacing =10.6 Å) for $[PEG_{10k}]_{50}$-$[PCL_{1k}]_{50}$ + 20% POSS blend when compared with the same peak for pure POSS-diol monomer (7.9°, d spacing = 11.1 Å). This could be due to some change in crystal lattice caused by the THF-solution casting process or by the architectural difference associated with backbone tethering in the TPU case. However, in-depth X-ray analysis pertaining to the change in crystal lattice is beyond the scope of this Article. Interestingly, a similar observation is also made for the multiblock TPUs covalently incorporating POSS moieties, that is, $[PEG_{10k}]_{50}$-$[PCL_{1k}]_{30}$-$[POSS]_{20}$ and $[PEG_{1k}]_{50}$-$[PCL_{1k}]_{30}$-$[POSS]_{20}$. The diffraction peaks related to POSS crystalline domain are also centered at d spacing of 10.7 Å in both samples, as shown in traces (v) and (vi) in Figure 2. However, the intensities of the diffraction peaks are lower, and the peaks are broader than that in the physical blending counterpart. This means that the physically blended sample could feature the POSS-rich domains with higher crystallinity and larger crystal size in the same loading. These results are consistent with our DSC observations. Besides, $[PEG_{10k}]_{50}$-$[PCL_{1k}]_{30}$-$[POSS]_{20}$ indicates another two strong characteristic peaks ascribed to 120 and $1\bar{3}2$ reflection peaks of PEG monoclinic unit. By comparison, $[PEG_{1k}]_{50}$-$[PCL_{1k}]_{30}$-$[POSS]_{20}$ only shows an amorphous halo due to the low molecular weights of PEG (1 kg/mol) and PCL (1.25 kg/mol) building blocks. Accordingly, this sample is elastomeric.

WAXS observations thus provide evidence that hydrophilic PEG blocks and hydrophobic PCL blocks and POSS macromers can each form individual crystalline microstructures in the multiblock thermoplastic polyurethanes (TPUs) due to microphase separation driven by thermodynamic incompatibility. With the same loading of POSS moieties, the physically blending sample featured POSS-rich domains with higher crystallinity and larger crystal size than the counterparts covalently incorporating POSS moieties.

In our PCL-PEG-based TPUs system, the hydrophilic PEG blocks were hydrated by water molecules, leading to mass gain and volumetric expansion. This swelling was limited by the presence of hydrophobic PCL- and POSS-rich domains. It was found that the water uptake of the TPUs increases with increasing PEG content, as shown in Table 2. Also, the water uptake depended on the molecular weight of PEG-diol blocks. In particular, the water uptake of $[PEG_{1k}]_{50}$-$[PCL_{1k}]_{30}$-$[POSS]_{20}$ was 70.7%, significantly lower than the other TPUs studied in this Article, the water uptake of which spanned from 164.4 to 182.0%. This is understood by the fact that the shorter PEG chain length in $[PEG_{1k}]_{50}$-$[PCL_{1k}]_{30}$-$[POSS]_{20}$ may lead to higher density and interconnectivity of the hydrophobic POSS domains, which serve as the physical cross-links of the hydrogel in the water-swollen state, so as to suppress the swelling and water uptake of the hydrogel.

Given that the POSS polyurethanes were designed to be mechanically robust, the ultimate mechanical properties were probed. Representative stress−strain curves of all five samples are provided in Figure 3, and the tensile properties are summarized in Table 3. Generally speaking, all of the samples exhibited extension behavior typical of semicrystalline polymers,[49,50] except $[PEG_{1k}]_{50}$-$[PCL_{1k}]_{30}$-$[POSS]_{20}$, which had much lower crystallinity than the others. Each sample displayed steep linear slopes at small strains, culminating in a yield point at a strain of ~20%. Following this yield point, the materials could be stretched further with plastic-like deformation, followed up by strain-hardening to an extension of 1200%, the maximum extension limit of our instrument for sample with this specific dimension. In contrast, $[PEG_{1k}]_{50}$-$[PCL_{1k}]_{30}$-$[POSS]_{20}$ displays characteristic elastomeric deformation.[50,51]

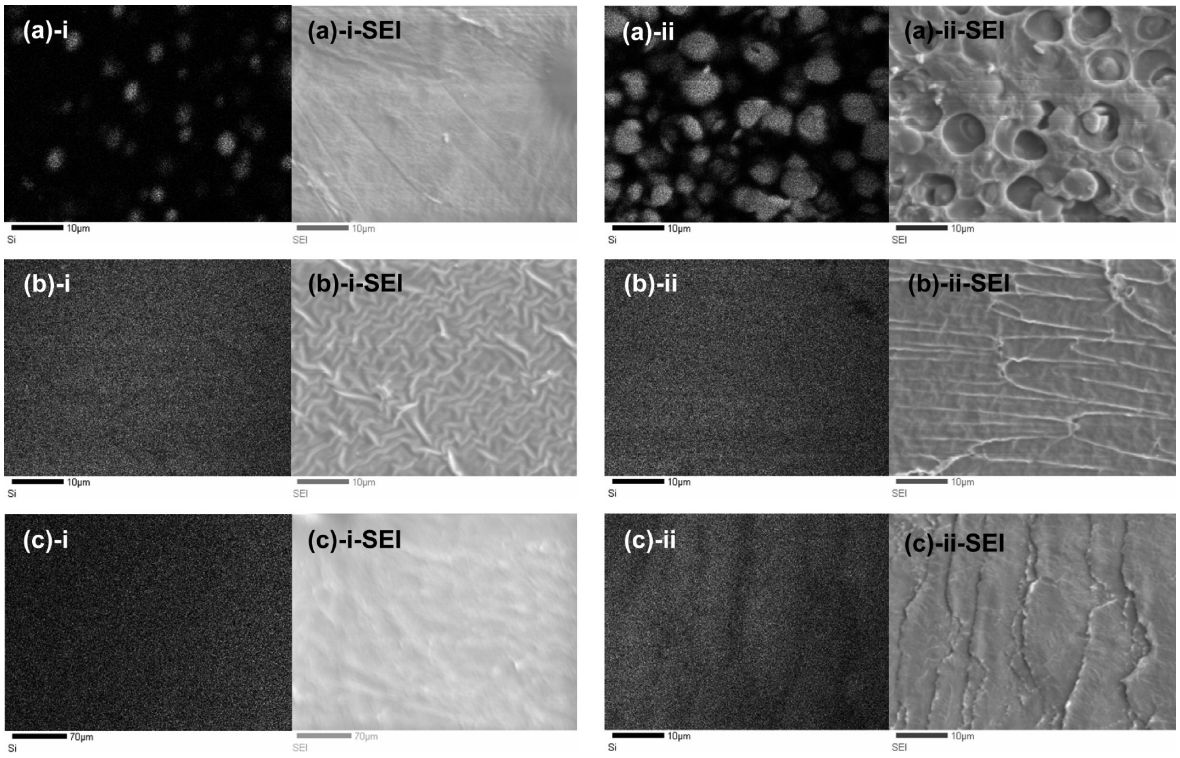

Figure 9. Surface silicon maps for: (a) $[PEG_{10k}]_{50}$-$[PCL_{1k}]_{50}$ + 20 wt % POSS: (i) swelled/dried and (ii) in lipase for 8 days; (b) $[PEG_{1k}]_{50}$-$[PCL_{1k}]_{30}$-$[LP]_{20}$: (i) swelled/dried and (ii) in lipase for 22 days; (c) $[PEG_{10k}]_{50}$-$[PCL_{1k}]_{30}$-$[LP]_{20}$: (i) swelled/dried and (ii) in lipase for 22 days obtained by wavelength dispersive X-ray spectroscopy (WDS). (a)-i-SEI, (a)-ii-SEI, (b)-i-SEI, (b)-ii-SEI, (c)-i-SEI, and (c)-ii-SEI are the corresponding SEI images of each element map.

As displayed in Figure 3, the yield point for necking of the $[PEG_{10k}]_{50}$-$[PCL_{1k}]_{50}$ was 4.6 MPa and 20% strain. This tensile yield for the TPU was followed by a period of elongation up to 670% strain at a relative constant stress of 4.4 MPa. As the material continued to undergo constant strain, an upturn in the stress after the 670% strain point was observed, indicating the onset of strain-hardening region that continued in the TPU. Compared with pure $[PEG10k]_{50}$-$[PCL1k]_{50}$, the physically blended samples, $[PEG_{10k}]_{50}$-$[PCL_{1k}]_{50}$ + 20% POSS, showed higher elastic modulus and yield stress. This is understood as the fact that POSS inclusion can enhance the modulus and strengthen the resulting nanocomposites.[52] The Young's modulus and yield stress of $[PEG_{10k}]_{50}$-$[PCL_{1k}]_{30}$-$[POSS]_{20}$ are higher than the $[PEG_{10k}]_{50}$-$[PCL_{1k}]_{50}$ + 20% POSS due to stronger chemical bonding among the three building blocks in the former material.

Enzymatic Degradation. Figure 4a exhibits the influence of POSS incorporation on mass, molecular weight, and water uptake of multiblock TPUs and $[PCL_{42k}]_{100}$ during enzymatic degradation. Highly crystalline PCL films with the same thickness as that used in the present study were previously reported to totally degrade in 4 days in the presence of *Pseudomonas* lipase,[15,16] consistent with our results. As compared with $[PCL_{42k}]_{100}$, PCL-PEG multiblock TPUs (50 wt % hydrophilic PEG block) showed a significantly lower enzymatic degradation rate. For the sample with 20 wt % POSS physically blended into the neat PCL-PEG multiblock TPUs, its enzymatic degradation time (the time points when the films broke into tiny pieces and the mass measurement for which is beyond our capability) significantly increased from 7 to 14 days. More surprisingly, the two TPUs covalently incorporating POSS moieties, $[PEG_{10k}]_{50}$-$[PCL_{1k}]_{30}$-$[POSS]_{20}$ and $[PEG_{1k}]_{50}$-$[PCL_{1k}]_{30}$-$[POSS]_{20}$, showed nearly no mass loss, except a very small portion of mass loss in the initial stage, within our experimental time range. Their enzymatic degradation behavior also seemed to be independent of PEG molecular weight. The normalized number-average molecular weight (M_n) for $[PCL_{42k}]_{100}$, $[PEG_{10k}]_{50}$-$[PCL_{1k}]_{50}$, and $[PEG_{10k}]_{50}$-$[PCL_{1k}]_{50}$ + 20% POSS showed an obvious decrease during degradation (Figure 4b). M_n for $[PCL_{42k}]_{100}$ and $[PEG_{10k}]_{50}$-$[PCL_{1k}]_{50}$ lost 40% after 4 and 8 d degradation, respectively, despite >90% weight loss. This is consistent with a modified surface erosion mechanism by enzyme, coupled to some bulk degradation. The measured decrease in the M_n of these three polymers could be attributed to residual polymer degradation products remaining on the polymer surface after degradation due to water-solubility limitations. The GPC test further showed that the molecular weight of the two TPUs covalently incorporating POSS moieties remained nearly constant for the duration of the study. M_n remaining profiles of PCL-PEG-based multiblock TPUs and $[PCL_{42k}]_{100}$ during enzymatic degradation can be found in the Supporting Information (Figure S3).

Swelling (water uptake) of all materials during degradation is shown in Figure 4c. The three samples with significant mass loss exhibited increasing water uptake during lipase incubation, consistent with some bulk degradation and molecular weight loss observed in Figure 4b. The two TPUs with covalently incorporated POSS showed no change in water uptake for 22 days.

^{1}H NMR was used to detect the changes in the chemical composition of four TPUs during the degradation by calculating the ratio of the peak areas assigned to PEG and PCL blocks in the

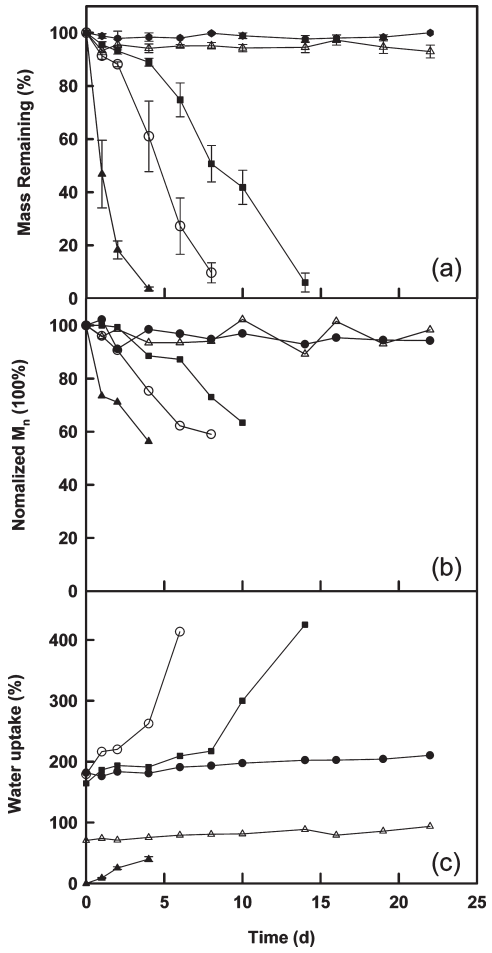

Figure 10. Surface silicon concentration profiles for: (a) $[PEG_{10k}]_{50}$-$[PCL_{1k}]_{50}$ + 20 wt % POSS: POSS particles (●) and matrix (○); (b) $[PEG_{1k}]_{50}$-$[PCL_{1k}]_{30}$-$[POSS]_{20}$; and (c) $[PEG_{10k}]_{50}$-$[PCL_{1k}]_{30}$-$[POSS]_{20}$ during enzymatic degradation, obtained by wavelength dispersive X-ray spectroscopy (WDS).

spectrum. The results are shown in Figure 5. It is found that EG/CL of all TPUs did not exhibit significant changes during lipase incubation, whether or not the materials showed mass loss. This initially surprising observation can be understood by considering that PCL can be degraded by lipase and that the remaining PEG and PEG-rich segments at the surface can easily escape from the surface by dissolution. The net effect was relative stability of the chemical compositions of the multiblock copolymers during degradation.

The phase behavior and thermal transitions of all samples also did not exhibit significant changes after enzyme incubation, as revealed by DSC. As-cast films were put into PBS buffer for 1 day as control (referred to as swelled/dried films). The heat flow traces shown are from first heating runs to assess the degraded state directly. Figure 6 shows the first heating curves of $[PCL_{42k}]_{100}$ and multiblock TPUs before and after enzyme incubation, whereas Table S1 of the Supporting Information summarizes their thermal property changes. We found that T_g, T_m, and ΔH_m for all segments did not change significantly as a result of enzyme incubation. The main melting peaks, which are ~50 °C in all four samples with higher crystallinity (Figure 5a,b,d,e), became more intense after lipase incubation, which could be attributed to the subsequent crystallization of amorphous areas and crystallite defects.[25]

Mechanical properties of all TPUs remain almost constant throughout enzyme incubation. The representative stress−strain curves for all materials before and after enzyme incubation are shown in Figure 7, and the tensile properties are summarized in Table S2 of the Supporting Information. For degraded samples, that is, $[PEG_{10k}]_{50}$-$[PCL_{1k}]_{50}$, $[PEG_{10k}]_{50}$-$[PCL_{1k}]_{50}$ + 20 wt % POSS, and $[PCL_{42k}]_{100}$, specific degradation times (6, 8, and 1 day, respectively) were picked for mechanical evaluation. Samples after those time points broke into small pieces, and tensile testing became impossible. With that restriction, we observed that the Young's modulus of all materials did not deteriorate but increased slightly after the enzymatic degradation test, resulting from the subsequent crystallization mentioned above. As the degradation progressed, the thickness of the three degraded samples decreased, resulting in a reduced signal-to-noise ratio for the stress signal of the stress−strain curves.

The surface morphology of the enzymatically degraded polyurethanes was investigated by SEM analysis and was compared with the TPUs films soaked in PBS for 1 day and dried (Figure 8). Compared with swelled/dried controls, all TPUs and $[PCL_{42k}]_{100}$ exhibited uniform rough surface following exposure to lipase. This indicates that all TPUs were eroded by a surface-limited mechanism when exposed to lipase, typical of enzymatic attack.[44] In the case of $[PEG_{10k}]_{50}$-$[PCL_{1k}]_{50}$ + 20 wt % POSS, some spherical particulates appeared on the surface of swelled/dried samples (Figure 8b−i). We reason that the material was softened during incubation and showed restructuring during drying, whereas the weak bonding between POSS and the bulk TPUs led to surface disintegration. After being incubated in enzyme for 10 days, this physically blended system showed porous structures on the surface, with the diameters of spherical particles being 5−10 μm (Figure 8b-ii). In contrast, we did not find this morphology in covalent-bonding systems (Figure 8c-ii,d-ii). Previously, we mentioned that the chemical composition and bulk mechanical properties of all degraded materials remained almost constant during enzyme incubation, which is in agreement with a surface erosion mechanism shown by SEM here.

The surfaces of the two TPUs covalently bonded with POSS also showed erosion, which is consistent with their initial mass loss profiles (Figure 4a). The surface of $[PEG_{1k}]_{50}$-$[PCL_{1k}]_{30}$-$[POSS]_{20}$ appeared smoother than that of $[PEG_{10k}]_{50}$-$[PCL_{1k}]_{30}$-$[POSS]_{20}$, as a result of lipase exposure (Figure 8c-ii,d-ii). The difference in surface topography is postulated to result from differences in crystallinity. $[PEG_{1k}]_{50}$-$[PCL_{1k}]_{30}$-$[POSS]_{20}$, the elastomeric sample with amorphous soft segment, was relatively soft compared with its counterpart, so we reason that the roughed surface resulting from enzyme attack got easily restructured during drying process, leading to a smoother surface.

Finally, wavelength dispersive X-ray spectrometry (WDS) was employed to investigate the distribution of POSS on the surface, as influenced by degradation. For the silicon maps shown in Figure 9, the gray scale represents the Si concentration on the surface; that is, the brighter parts on the images indicate higher silicon concentration on the surface. Figure 9a−i shows that, as prepared, POSS aggregated into micrometer-sized domains in $[PEG_{10k}]_{50}$-$[PCL_{1k}]_{50}$ + 20% POSS. When this polymer film was exposed to the lipase solution, POSS aggregated further on the surface (Figure 9a-ii). The brighter part, which is believed to be the POSS aggregates, corresponds well to

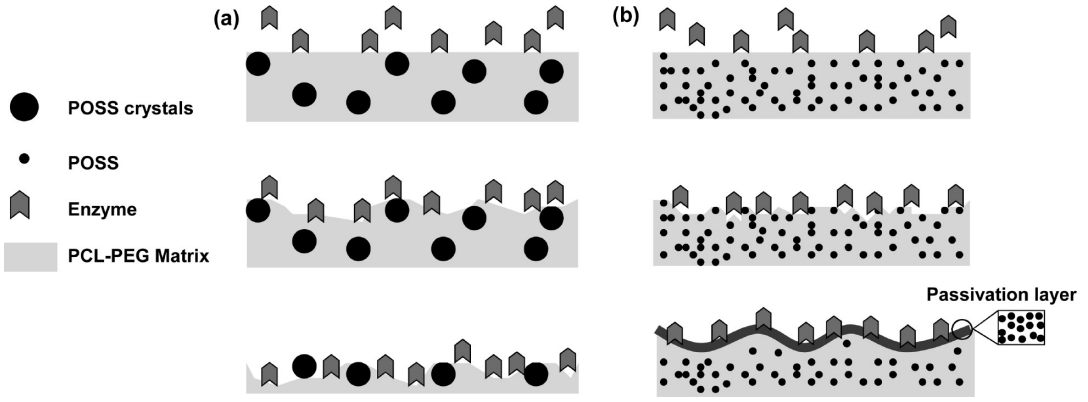

Figure 11. Proposed surface passivation mechanism for PCL-PEG-based TPUs: (a) physically blended with POSS and (b) covalently bonded with POSS.

the particles observed in the corresponding SEI (secondary electron images) (Figure 9a-ii-SEI). At the same POSS loading, the two TPUs covalently bonded with POSS exhibited uniform dispersed POSS domains before and after enzyme incubation (Figure 8b-i,ii and c-i,ii).

For each sample, 10 different locations were scanned by WDS, and the percentage of silicon element was calculated. Average values for these ten locations are reported herein, with the error bars indicating the standard deviation (Figure 10). As mentioned above, after enzymatic degradation, $[PEG_{10k}]_{50}$-$[PCL_{1k}]_{50}$ + 20% POSS exhibited a particle/matrix morphology, so the Si concentration of particle and matrix were both characterized. We found that silicon concentration is significantly higher in the particles than in the matrix (Figure 10a), which corresponds to the silicon concentration map of this material. The silicon concentration of both the particles and the matrix remained almost constant from day 2 to day 8 of lipase degradation. For the other two covalently bonding systems, $[PEG_{1k}]_{50}$-$[PCL_{1k}]_{30}$-$[POSS]_{20}$ and $[PEG_{1k}]_{50}$-$[PCL_{1k}]_{30}$-$[POSS]_{20}$, (Figure 10b,c), silicon concentration increased slightly from 2.2 to 3.9 wt % and from 2.2 to 3.3 wt %, respectively, as the incubation time transpired. Converting the silicon weight percentage to POSS weight percentage, the POSS concentrations on the surface of these two materials before degradation were both found, coincidentally, to be 9.2 wt %, lower than the results obtained by ^{1}H NMR (Table 1), which are 21 and 15 wt % respectively. We postulate that during film casting POSS became somewhat buried beneath the surface, a somewhat unexpected result considering the hydrophobicity of POSS and likely preference for the liquid/air interface.

Combining SEM and WDS observations, we propose a surface passivation mechanism for different degradation behaviors of both physically blending system and covalently bonding system with POSS during enzyme incubation. When the physically blended system (Figure 11a) was exposed to enzyme, the PCL-PEG segments eroded, leading to enhancement of large POSS domains at the surface. This coarse microstructure is apparently unable to inhibit enzymatic hydrolysis, although it does retard degradation to some degree. In contrast, enzymatic degradation of the covalently bonded POSS system led initially to PCL-PEG segment erosion that became suppressed as nanodispersed POSS formed a homogeneous passivation layer that was effective in preventing further enzymatic degradation from occurring. Such a passivation mechanism consistent with all of our findings is shown in schematic form in Figure 11b.

CONCLUSIONS

Multiblock thermoplastic polyurethanes have been synthesized from lysine-diisocyanate (LDI) with PCL-diol (1.25 kg/mol), POSS-diol, and PEG (1.0 and 10.0 kg/mol) using a one-step technique. To discern importance of POSS covalent incorporation on biostability, we prepared a physical blend of POSS and PCL-PEG multiblock TPUs and a pure PCL-PEG multiblock TPUs without any POSS incorporation. Both DSC and WAXS observations indicated microphase separation between hydrophilic PEG blocks and hydrophobic PCL-diol/POSS-diol due to thermodynamic incompatibility. Three week enzymatic degradation experiments showed that POSS incorporation significantly suppressed in vitro degradation of PCL-based multiblock TPUs. The multiblock TPUs covalently tethered with 20 wt % POSS moieties showed suppression of mass loss and molecular weight decrease within, whereas the physically blended POSS samples only retarded enzymatic hydrolysis kinetics. Calorimetric, spectroscopic, mechanical, and microscopic observations revealed that all TPUs were surface-eroded by enzymatic attack in which the chemical composition and the bulk mechanical properties of all TPUs exhibiting little changes. We propose a surface passivation mechanism to explain the protection of POSS-containing TPUs from enzymatic degradation. These striking results provide a new strategy to design novel long-term biostable polyurethane implants.

ASSOCIATED CONTENT

Supporting Information. NMR spectrum for a sample polymer, $[PEG_{10k}]_{50}$-$[PCL_{1k}]_{30}$-$[POSS]_{20}$, with characteristic peaks labeled; DSC second heating traces for PCL-PEG-based TPUs showing POSS melting peaks (i) $[PEG_{10k}]_{50}$-$[PCL_{1k}]_{50}$ and (ii) $[PEG_{10k}]_{50}$-$[PCL_{1k}]_{50}$ + 20 wt % POSS; (iii) $[PEG_{1k}]_{50}$-$[PCL_{1k}]_{30}$-$[POSS]_{20}$; and (iv) $[PEG_{10k}]_{50}$-$[PCL_{1k}]_{30}$-$[POSS]_{20}$; number-average molecular weight (M_n) remaining profiles of PCL-PEG-based multiblock TPUs and $[PCL_{42k}]_{100}$ during enzymatic degradation; thermal properties of PCL-PEG-based multiblock TPUs and $[PCL_{42k}]_{100}$ before and after lipase incubation; and mechanical properties of PCL-PEG-based multiblock TPUs and $[PCL_{42k}]_{100}$ before and after lipase incubation.

This material is available free of charge via the Internet at http://pubs.acs.org.

AUTHOR INFORMATION

Corresponding Author

*E-mail: ptmather@syr.edu. Tel: (315) 443-8760. Fax: (315) 443-9175.

Author Contributions

[†]These authors contributed equally.

ACKNOWLEDGMENT

We gratefully acknowledge the financial support of the New York State Office of Science, Technology and Academic Research (NYSTAR) (CON01587). We also thank Mr. Michael Cheatham from Department of Earth Science in Syracuse University for WDS experiments.

REFERENCES

(1) Stokes, K.; McVenes, R.; Anderson, J. M. *J. Biomater. Appl.* **1995**, *9*, 321–354.
(2) Zdrahala, R. J.; Zdrahala, I. J. *J. Biomater. Appl.* **1999**, *14*, 67–90.
(3) Pinchuk, L. *J. Biomater. Sci., Polym. Ed.* **1994**, *6*, 225–267.
(4) Boretos, J. W.; Pierce, W. S. *Science* **1967**, *158*, 1481–1482.
(5) Seifalian, A. M.; Salacinski, H. J.; Tiwari, A.; Edwards, A.; Bowald, S.; Hamilton, G. *Biomaterials* **2003**, *24*, 2549–2557.
(6) Salacinski, H. J.; Tai, N. R.; Carson, R. J.; Edwards, A.; Hamilton, G.; Seifalian, A. M. *J. Biomed. Mater. Res.* **2002**, *59*, 207–218.
(7) Anderson, J. M.; Hiltner, A.; Wiggins, M. J.; Schubert, M. A.; Collier, T. O.; Kao, W. J.; Mathur, A. B. *Polym. Int.* **1998**, *46*, 163–171.
(8) Armani, D. K.; Liu, C. *J. Micromech. Microeng.* **2000**, *10*, 80–84.
(9) Harris, J. M.; Chess, R. B. *Nat. Rev. Drug Discovery* **2003**, *2*, 214–221.
(10) Lefebvre, F.; David, C.; Vanderwauven, C. *Polym. Degrad. Stab.* **1994**, *45*, 347–353.
(11) Akahori, S.; Osawa, Z. *Polym. Degrad. Stab.* **1994**, *45*, 261–265.
(12) DeKesel, C.; VanderWauven, C.; David, C. *Polym. Degrad. Stab.* **1997**, *55*, 107–113.
(13) Fukuzaki, H.; Yoshida, M.; Asano, M.; Kumakura, M.; Mashimo, T.; Yuasa, H.; Imai, K.; Yamanaka, H. *Polymer* **1990**, *31*, 2006–2014.
(14) Mochizuki, M.; Hirano, M.; Kanmuri, Y.; Kudo, K.; Tokiwa, Y. *J. Appl. Polym. Sci.* **1995**, *55*, 289–296.
(15) Gan, Z. H.; Liang, Q. Z.; Zhang, J.; Jing, X. B. *Polym. Degrad. Stab.* **1997**, *56*, 209–213.
(16) Gan, Z. H.; Yu, D. H.; Zhong, Z. Y.; Liang, Q. Z.; Jing, X. B. *Polymer* **1999**, *40*, 2859–2862.
(17) Liu, L. J.; Li, S. M.; Garreau, H.; Vert, M. *Biomacromolecules* **2000**, *1*, 350–359.
(18) Kobayashi, S.; Uyama, H.; Takamoto, T. *Biomacromolecules* **2000**, *1*, 3–5.
(19) Li, S. M.; Garreau, H.; Pauvert, B.; McGrath, J.; Toniolo, A.; Vert, M. *Biomacromolecules* **2002**, *3*, 525–530.
(20) Yeganeh, H.; Jamshidi, H.; Jamshidi, S. *Polym. Int.* **2007**, *56*, 41–49.
(21) Desai, N. P.; Hubbell, J. A. *J. Biomed. Mater. Res.* **1991**, *25*, 829–843.
(22) Scott, M. D.; Murad, K. L. *Curr. Pharm. Des.* **1998**, *4*, 423–438.
(23) Csucs, G.; Michel, R.; Lussi, J. W.; Textor, M.; Danuser, G. *Biomaterials* **2003**, *24*, 1713–1720.
(24) Fromstein, J. D.; Woodhouse, K. A. *J. Biomater. Sci., Polym. Ed.* **2002**, *13*, 391–406.
(25) Li, S. M.; Garreau, H.; Vert, M.; Petrova, T.; Manolova, N.; Rashkov, I. *J. Appl. Polym. Sci.* **1998**, *68*, 989–998.
(26) Zhou, S. B.; Deng, X. M.; Yang, H. *Biomaterials* **2003**, *24*, 3563–3570.
(27) He, F.; Li, S. M.; Vert, M.; Zhuo, R. X. *Polymer* **2003**, *44*, 5145–5151.
(28) Gan, Z. H.; Jim, T. F.; Li, M.; Yuer, Z.; Wang, S. G.; Wu, C. *Macromolecules* **1999**, *32*, 590–594.
(29) Cohn, D.; Stern, T.; Gonzalez, M. F.; Epstein, J. *J. Biomed. Mater. Res.* **2002**, *59*, 273–281.
(30) Huang, M. H.; Li, S. M.; Hutmacher, D. W.; Schantz, J. T.; Vacanti, C. A.; Braud, C.; Vert, M. *J. Biomed. Mater. Res., Part A* **2004**, *69A*, 417–427.
(31) Im, S. J.; Choi, Y. M.; Subrarnanyarn, E.; Huh, K. M.; Park, K. *Macromol. Res.* **2007**, *15*, 363–369.
(32) Skarja, G. A.; Woodhouse, K. A. *J. Biomater. Sci., Polym. Ed.* **1998**, *9*, 271–295.
(33) Skarja, G. A.; Woodhouse, K. A. *J. Appl. Polym. Sci.* **2000**, *75*, 1522–1534.
(34) Skarja, G. A.; Woodhouse, K. A. *J. Biomater. Sci., Polym. Ed.* **2001**, *12*, 851–873.
(35) Gunatillake, P. A.; Martin, D. J.; Meijs, G. F.; McCarthy, S. J.; Adhikari, R. *Aust. J. Chem.* **2003**, *56*, 545–557.
(36) Wu, J.; Mather, P. T. *Polym. Rev.* **2009**, *49*, 25–63.
(37) Hsiao, B. S.; White, H.; Rafailovich, M.; Mather, P. T.; Jeon, H. G.; Phillips, S.; Lichtenhan, J.; Schwab, J. *Polym. Int.* **2000**, *49*, 437–440.
(38) Fu, B. X.; Hsiao, B. S.; Pagola, S.; Stephens, P.; White, H.; Rafailovich, M.; Sokolov, J.; Mather, P. T.; Jeon, H. G.; Phillips, S.; Lichtenhan, J.; Schwab, J. *Polymer* **2001**, *42*, 599–611.
(39) Knight, P. T.; Lee, K. M.; Qin, H.; Mather, P. T. *Biomacromolecules* **2008**, *9*, 2458–2467.
(40) Guo, Q. Y.; Knight, P. T.; Mather, P. T. *J. Controlled Release* **2009**, *137*, 224–233.
(41) Knight, P. T.; Kirk, J. T.; Anderson, J. M.; Mather, P. T. *J. Biomed. Mater. Res., Part A* **2010**, *94A*, 333–343.
(42) Wu, J.; Ge, Q.; Mather, P. T. *Macromolecules* **2010**, *43*, 7637–7649.
(43) Kannan, R. Y.; Salacinski, H. J.; Odlyha, M.; Butler, P. E.; Seifalian, A. M. *Biomaterials* **2006**, *27*, 1971–1979.
(44) Christenson, E. M.; Patel, S.; Anderson, J. M.; Hiltner, A. *Biomaterials* **2006**, *27*, 3920–3926.
(45) Tanzi, M. C.; Mantovani, D.; Petrini, P.; Guidoin, R.; Laroche, G. *J. Biomed. Mater. Res.* **1997**, *36*, 550–559.
(46) Mathur, A. B.; Collier, T. O.; Kao, W. J.; Wiggins, M.; Schubert, M. A.; Hiltner, A.; Anderson, J. M. *J. Biomed. Mater. Res.* **1997**, *36*, 246–257.
(47) Waddon, A. J.; Zheng, L.; Farris, R. J.; Coughlin, E. B. *Nano Lett.* **2002**, *2*, 1149–1155.
(48) Qiu, Z. B.; Ikehara, T.; Nishi, T. *Polymer* **2003**, *44*, 3101–3106.
(49) Foks, J.; Janik, H.; Russo, R. *Eur. Polym. J.* **1990**, *26*, 309–314.
(50) Young, R. J.; Lovell, P. A. *Introduction to Polymers*; Chapman & Hall: London: 1991; p 394.
(51) Petrovic, Z. S.; Ferguson, J. *Prog. Polym. Sci.* **1991**, *16*, 695–836.
(52) Petrovic, Z. S.; Javni, I.; Waddon, A.; Banhegyi, G. *J. Appl. Polym. Sci.* **2000**, *76*, 133–151.